
Poincaré Embeddings for Learning Hierarchical Representations

Maximilian Nickel
 Facebook AI Research
 maxn@fb.com

Douwe Kiela
 Facebook AI Research
 dkiele@fb.com

Abstract

Representation learning has become an invaluable approach for learning from symbolic data such as text and graphs. However, while complex symbolic datasets often exhibit a latent hierarchical structure, state-of-the-art methods typically learn embeddings in Euclidean vector spaces, which do not account for this property. For this purpose, we introduce a new approach for learning hierarchical representations of symbolic data by embedding them into hyperbolic space – or more precisely into an n -dimensional Poincaré ball. Due to the underlying hyperbolic geometry, this allows us to learn parsimonious representations of symbolic data by simultaneously capturing hierarchy and similarity. We introduce an efficient algorithm to learn the embeddings based on Riemannian optimization and show experimentally that Poincaré embeddings outperform Euclidean embeddings significantly on data with latent hierarchies, both in terms of representation capacity and in terms of generalization ability.

1 Introduction

Learning representations of symbolic data such as text, graphs and multi-relational data has become a central paradigm in machine learning and artificial intelligence. For instance, word embeddings such as WORD2VEC [17], GLOVE [22] and FASTTEXT [4] are widely used for tasks ranging from machine translation to sentiment analysis. Similarly, embeddings of graphs such as latent space embeddings [13] and NODE2VEC [11] have found important applications for community detection and link prediction in social networks. Embeddings of multi-relational data such as RESCAL [19] and TRANSE [6] are being used for knowledge graph completion and relation extraction.

Typically, the objective of embedding methods is to organize symbolic objects (e.g., words, entities, concepts) in a way such that their similarity in the embedding space reflects their semantic or functional similarity. For this purpose, the similarity of objects is usually measured either by their distance or by their inner product in the embedding space. For instance, Mikolov et al. [17] embed words in \mathbb{R}^d such that their inner product is maximized when words co-occur within similar contexts in text corpora. This is motivated by the distributional hypothesis [12, 9], i.e., that the meaning of words can be derived from the contexts in which they appear. Similarly, Hoff et al. [13] embed social networks such that the distance between social actors is minimized if they are connected in the network. This reflects the homophily property found in many real-world networks, i.e. that similar actors tend to associate with each other.

Although current embedding methods have proven successful in numerous applications, they suffer from a fundamental limitation: their ability to model complex patterns is inherently bounded by the dimensionality of the embedding space. For instance, Nickel et al. [20] showed that linear embeddings of graphs can require a prohibitively large dimensionality to model certain types of relationships. Although non-linear embeddings can mitigate this problem [7], the dimensionality that is required to model complex patterns in graphs can still be computationally infeasible. As a consequence, no method yet exists that is able to compute embeddings of large graph-structured data – such as social

networks, knowledge graphs or taxonomies – without loss of information. Since the ability to express information is a precondition for learning and generalization, it is therefore important to increase the representation capacity of embedding methods such that they realistically can be used to model complex patterns on a large scale.

In this work, we intend to mitigate this problem for a certain class of symbolic data, i.e., large datasets whose objects can be organized according to a latent hierarchy – a property that is inherent in many complex datasets. For instance, the existence of power-law distributions in datasets can often be traced back to hierarchical structures [23]. Prominent examples of power-law distributed data include natural language (Zipf’s law [29]) and scale-free networks such as social and semantic networks [25]. Similarly, the empirical analysis of Adcock et al. [1] indicated that many real-world networks exhibit an underlying tree-like structure.

To exploit this structural property for learning more efficient representations, we propose to compute embeddings not in Euclidean but in hyperbolic space, i.e., space with constant negative curvature. Informally, hyperbolic space can be thought of as a continuous version of trees and as such it is naturally equipped to model hierarchical structures. For instance, it has been shown that any finite tree can be embedded into a finite hyperbolic space such that distances are preserved approximately [10]. We base our approach on a particular model of hyperbolic space, i.e., the Poincaré ball model, as it is well-suited for gradient-based optimization. This allows us to develop an efficient algorithm for computing the embeddings based on Riemannian optimization, which is easily parallelizable and scales to large datasets. Experimentally, we show that our approach can provide high quality embeddings of large taxonomies – both with and without missing data. Moreover, we show that embeddings trained on WORDNET provide state-of-the-art performance for lexical entailment. On collaboration networks, we also show that Poincaré embeddings are successful in predicting links in graphs where they outperform Euclidean embeddings, especially in low dimensions.

The remainder of this paper is organized as follows: In Section 2 we briefly review hyperbolic geometry and discuss related work regarding hyperbolic embeddings. In Section 3 we introduce Poincaré embeddings and discuss how to compute them. In Section 4 we evaluate our approach on tasks such as taxonomy embedding, link prediction in networks and predicting lexical entailment.

2 Embeddings and Hyperbolic Geometry

Hyperbolic geometry is a non-Euclidean geometry which studies spaces of constant negative curvature. It is, for instance, associated with Minkowski spacetime in special relativity. In network science, hyperbolic spaces have started to receive attention as they are well-suited to model hierarchical information. For instance, consider the task of embedding a tree into a metric space such that its structure is reflected in the embedding. A regular tree with branching factor b has $(b + 1)b^{\ell-1}$ nodes at level ℓ and $((b + 1)b^\ell - 2)/(b - 1)$ nodes on a level less or equal than ℓ . Hence, the number of children grows exponentially with their distance to the root of the tree. In hyperbolic geometry this kind of tree structure can be modeled easily in two dimensions: nodes that are *exactly* ℓ levels below the root are placed on a sphere in hyperbolic space with radius $r \propto \ell$ and nodes that are *less than* ℓ levels below the root are located within this sphere. This type of construction is possible as hyperbolic disc area and circle length grow exponentially with their radius.¹ An example of this construction is shown in Figure 1b. Intuitively, hyperbolic spaces can be thought of as continuous versions of trees or vice versa, trees can be thought of as "discrete hyperbolic spaces" [16]. Note that a similar construction is not possible in \mathbb{R}^2 as circle length $(2\pi r)$ and disc area $(2\pi r^2)$ grow only linearly and quadratically with regard to r in Euclidean geometry. Instead, it is necessary to increase the dimensionality of the embedding to model increasingly complex hierarchies. As the number of parameters increases, this can lead to computational problems in terms of runtime and memory complexity as well as to overfitting.

Due to these properties, hyperbolic space has recently been considered for modeling complex networks such as communication networks and social networks. For instance, Kleinberg [15] introduced hyperbolic geometry for greedy routing in geographic communication networks. Similarly, Boguñá et al. [3] proposed hyperbolic embeddings of the AS Internet topology to perform greedy shortest

¹For instance, in a two dimensional hyperbolic space with constant curvature $K = -1$, the length of a circle is given as $2\pi \sinh r$ while the area of a disc is given as $2\pi(\cosh r - 1)$. Since $\sinh r = \frac{1}{2}(e^r - e^{-r})$ and $\cosh r = \frac{1}{2}(e^r + e^{-r})$, both disc area and circle length grow exponentially with r .

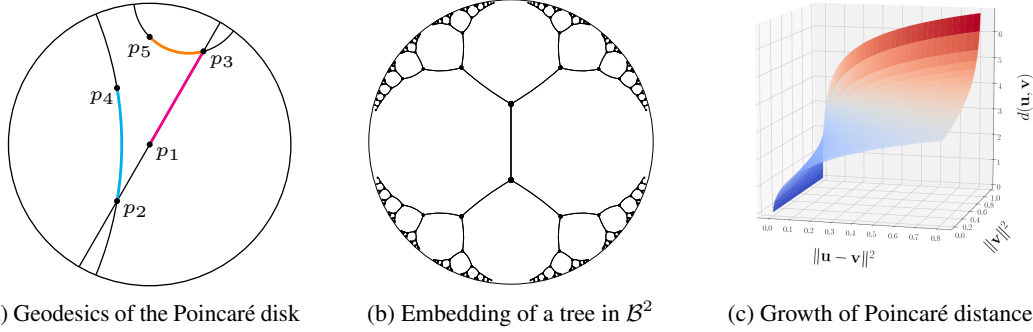


Figure 1: (a) Due to the negative curvature of \mathcal{B} , the distance of points increases exponentially (relative to their Euclidean distance) the closer they are to the boundary. (c) Growth of the Poincaré distance $d(\mathbf{u}, \mathbf{v})$ relative to the Euclidean distance and the norm of \mathbf{v} (for fixed $\|\mathbf{u}\| = 0.9$). (b) Embedding of a regular tree in \mathcal{B}^2 such that all line segments have equal length.

path routing in the embedding space. Krioukov et al. [16] developed a framework to model complex networks using hyperbolic spaces and discussed how typical properties such as heterogeneous degree distributions and strong clustering emerges by assuming an underlying hyperbolic geometry to these networks. Adcock et al. [1] proposed a measure based on Gromov’s δ -hyperbolicity [10] to characterize the tree-likeness of graphs.

3 Poincaré Embeddings

In the following, we are interested in finding embeddings of symbolic data such that their distance in the embedding space reflects their semantic similarity. We assume that there exists a latent hierarchy in which the symbols can be organized. We intend to reflect this hierarchy in the embedding space to improve over existing methods in two ways:

1. By inducing an appropriate bias on the structure of the embedding space, we aim at learning more parsimonious embeddings for superior generalization performance and decreased runtime and memory complexity.
2. By capturing the hierarchy explicitly in the embedding space, we aim at gaining additional insights about the relationships between symbols and the importance of individual symbols.

For these reasons – and motivated by the discussion in Section 2 – we embed symbolic data into hyperbolic space \mathbb{H} . In contrast to Euclidean space \mathbb{R} , there exist multiple, equivalent models of \mathbb{H} such as the Beltrami-Klein model, the hyperboloid model, and the Poincaré half-plane model. In the following, we will base our approach on the Poincaré ball model, as it is well-suited for gradient-based optimization.² In particular, let $\mathcal{B}^d = \{\mathbf{x} \in \mathbb{R}^d \mid \|\mathbf{x}\| < 1\}$ be the open d -dimensional unit ball, where $\|\cdot\|$ denotes the Euclidean norm. The Poincaré ball model of hyperbolic space corresponds then to the Riemannian manifold $(\mathcal{B}^d, g_{\mathbf{x}})$, i.e., the open unit ball equipped with the Riemannian metric tensor

$$g_{\mathbf{x}} = \left(\frac{2}{1 - \|\mathbf{x}\|^2} \right)^2 g^E,$$

where $\mathbf{x} \in \mathcal{B}^d$ and g^E denotes the Euclidean metric tensor. Furthermore, the distance between points $\mathbf{u}, \mathbf{v} \in \mathcal{B}^d$ is given as

$$d(\mathbf{u}, \mathbf{v}) = \text{arcosh} \left(1 + 2 \frac{\|\mathbf{u} - \mathbf{v}\|^2}{(1 - \|\mathbf{u}\|^2)(1 - \|\mathbf{v}\|^2)} \right) \quad (1)$$

²It can be seen easily that the distance function of the Poincaré ball in Equation (1) is differentiable. Hence, for this model, an optimization algorithm only needs to maintain the constraint that the norm of the embeddings is less than one. Other models of hyperbolic space however, would be more difficult to optimize, either due to the form of their distance function or due to the constraints that they introduce. For instance, the hyperboloid model is constrained to points where $\langle \mathbf{x}, \mathbf{x} \rangle = -1$, while the Beltrami-Klein model requires to compute the location of ideal points on the boundary $\partial\mathcal{B}$ of the unit ball to compute the distance between points.

The boundary of the ball is denoted by $\partial\mathcal{B}$. It corresponds to the sphere \mathcal{S}^{d-1} and is not part of the hyperbolic space, but represents infinitely distant points. Geodesics in \mathcal{B}^d are then circles that are orthogonal to $\partial\mathcal{B}$ (as well as all diameters). See Figure 1a for an illustration.

It can be seen from Equation (1), that the distance within the Poincaré ball changes smoothly with respect to the location of u and v . This locality property of the Poincaré distance is key for finding continuous embeddings of hierarchies. For instance, by placing the root node of a tree at the origin of \mathcal{B}^d it would have a relatively small distance to all other nodes as its Euclidean norm is zero. On the other hand, leaf nodes can be placed close to the boundary of the Poincaré ball as the distance grows very fast between points with a norm close to one. Furthermore, please note that Equation (1) is symmetric and that the hierarchical organization of the space is solely determined by the distance of points to the origin. Due to this self-organizing property, Equation (1) is applicable to data such as text and networks where the hierarchical order of objects is not specified in advance. Remarkably, Equation (1) allows us therefore to learn embeddings that simultaneously capture the hierarchy of objects (through their norm) as well as their similarity (through their distance).

Since a single hierarchical structure can already be represented in two dimensions, the Poincaré disk (\mathcal{B}^2) is typically used to represent hyperbolic geometry. In our method, we instead use the Poincaré ball (\mathcal{B}^d), for two main reasons: First, in many datasets such as text corpora, multiple latent hierarchies can co-exist, which can not always be modeled in two dimensions. Second, a larger embedding dimension can decrease the difficulty for an optimization method to find a good embedding (also for single hierarchies) as it allows for more degrees of freedom during the optimization process.

To compute Poincaré embeddings for a set of symbols $\mathcal{S} = \{x_i\}_{i=1}^n$, we are then interested in finding embeddings $\Theta = \{\theta_i\}_{i=1}^n$, where $\theta_i \in \mathcal{B}^d$. We assume we are given a problem-specific loss function $\mathcal{L}(\Theta)$ which encourages semantically similar objects to be close in the embedding space according to their Poincaré distance. To estimate Θ , we then solve the optimization problem

$$\Theta' \leftarrow \arg \min_{\Theta} \mathcal{L}(\Theta) \quad \text{s.t. } \forall \theta_i \in \Theta : \|\theta_i\| < 1. \quad (2)$$

We will discuss specific loss functions in Section 4.

3.1 Optimization

Since the Poincaré Ball has a Riemannian manifold structure, we can optimize Equation (2) via stochastic Riemannian optimization methods such as RSGD [5] or RSVRG [28]. In particular, let $\mathcal{T}_{\theta}\mathcal{B}$ denote the tangent space of a point $\theta \in \mathcal{B}^d$. Furthermore, let $\nabla_R \in \mathcal{T}_{\theta}\mathcal{B}$ denote the Riemannian gradient of $\mathcal{L}(\theta)$ and let ∇_E denote the Euclidean gradient of $\mathcal{L}(\theta)$. Using RSGD, parameter updates to minimize Equation (2) are then of the form

$$\theta_{t+1} = \mathfrak{R}_{\theta_t}(-\eta_t \nabla_R \mathcal{L}(\theta_t))$$

where \mathfrak{R}_{θ_t} denotes the retraction onto \mathcal{B} at θ and η_t denotes the learning rate at time t . Hence, for the minimization of Equation (2), we require the Riemannian gradient and a suitable retraction. Since the Poincaré ball is a conformal model of hyperbolic space, the angles between adjacent vectors are identical to their angles in the Euclidean space. The length of vectors however might differ. To derive the Riemannian gradient from the Euclidean gradient, it is sufficient to rescale ∇_E with the inverse of the Poincaré ball metric tensor, i.e., g_{θ}^{-1} . Since g_{θ} is a scalar matrix, the inverse is trivial to compute. Furthermore, since Equation (1) is fully differentiable, the Euclidean gradient can easily be derived using standard calculus. In particular, the Euclidean gradient $\nabla_E = \frac{\partial \mathcal{L}(\theta)}{\partial d(\theta, x)} \frac{\partial d(\theta, x)}{\partial \theta}$ depends on the gradient of \mathcal{L} , which we assume is known, and the partial derivatives of the Poincaré distance, which can be computed as follows: Let $\alpha = 1 - \|\theta\|^2$, $\beta = 1 - \|x\|^2$ and let

$$\gamma = 1 + \frac{2}{\alpha\beta} \|\theta - x\|^2 \quad (3)$$

The partial derivative of the Poincaré distance with respect to θ is then given as

$$\frac{\partial d(\theta, x)}{\partial \theta} = \frac{4}{\beta \sqrt{\gamma^2 - 1}} \left(\frac{\|x\|^2 - 2\langle \theta, x \rangle + 1}{\alpha^2} \theta - \frac{x}{\alpha} \right). \quad (4)$$

Since $d(\cdot, \cdot)$ is symmetric, the partial derivative $\frac{\partial d(x, \theta)}{\partial \theta}$ can be derived analogously. As retraction operation we use $\mathfrak{R}_{\theta}(v) = \theta + v$. In combination with the Riemannian gradient, this corresponds

then to the well-known natural gradient method [2]. Furthermore, to ensure that the embeddings remain within the Poincaré ball, we project them back into \mathcal{B} should their norm become larger than one. In summary, the full update is of the form

$$\boldsymbol{\theta}_{t+1} \leftarrow \text{proj} \left(\boldsymbol{\theta}_t - \eta_t \frac{(1 - \|\boldsymbol{\theta}_t\|^2)^2}{4} \nabla_E \right) \quad (5)$$

where

$$\text{proj}(\mathbf{x}) = \begin{cases} \mathbf{x}/\|\mathbf{x}\| - \varepsilon & \text{if } \|\mathbf{x}\| \geq 1 \\ \mathbf{x} & \text{otherwise.} \end{cases}$$

and where ε is a small constant to ensure numerical stability. In all experiments we used $\varepsilon = 10^{-5}$.

It can be seen from Equations (4) and (5) that this algorithm scales well to large datasets, as the update of a single embedding scales linearly in the embedding dimension. Moreover, it is straightforward to parallelize via methods such as Hogwild [24], as the updates are sparse (only a small number of embeddings are modified in an update) and collisions are very unlikely on large-scale data.

3.2 Training Details

In addition to the optimization procedure described in Section 3.1, we found that the following training details were helpful for obtaining good representations: First, we initialize all embeddings randomly from the uniform distribution $\mathcal{U}(-0.001, 0.001)$. This causes the embeddings to be initialized close to the origin of the Poincaré ball. Second, we found that a good initial angular layout can be helpful to find good embeddings. For this reason we train initially during a "burn-in" phase with a reduced learning rate η/c . In combination with initializing close to the origin, this can improve the angular layout without moving too far towards the boundary. In our experiments, we set $c = 10$ and the duration of the burn-in to 10 epochs.

4 Evaluation

In this section, we evaluate the quality of Poincaré embeddings for a variety of tasks, i.e., for the embedding of taxonomies, for link prediction in networks, and for modeling lexical entailment. In our evaluation, we compare the **Poincaré** distance as defined in Equation (1) to the following two distance functions:

Euclidean In all cases, we include the Euclidean distance $d(\mathbf{u}, \mathbf{v}) = \|\mathbf{u} - \mathbf{v}\|^2$. As the Euclidean distance is flat and symmetric, we expect that it requires a very large dimensionality to model the hierarchical structure of the data.

Translational For asymmetric data, we also include the score function $d(\mathbf{u}, \mathbf{v}) = \|\mathbf{u} - \mathbf{v} + \mathbf{r}\|^2$, as proposed by Bordes et al. [6] for modeling large-scale graph-structured data. For this score function, we also learn the global translation vector \mathbf{r} during training.

Note that the translational score function has, due to its asymmetry, more information about the nature of an embedding problem than a symmetric distance when the order of (\mathbf{u}, \mathbf{v}) indicates the hierarchy of elements. This is, for instance, the case for `is-a` (\mathbf{u}, \mathbf{v}) relations in taxonomies. For the Poincaré distance and the Euclidean distance we could randomly permute the order of (\mathbf{u}, \mathbf{v}) and obtain the identical embedding, while this is not the case for the translational score function. As such, it is not fully self-organizing and only applicable to data where this information is available.

4.1 Embedding Taxonomies

In the first set of experiments, we are interested in evaluating the ability of Poincaré embeddings to embed data with a clear hierarchical structure such as taxonomies. For this purpose, we conduct experiments on the WORDNET noun hierarchy [18] in two settings:

Reconstruction To evaluate representation capacity, we embed fully observed data and reconstruct it from the embedding. The reconstruction error in relation to the embedding dimension is then a measure for the capacity of the model.

Table 1: Experimental results on the transitive closure of the WORDNET noun hierarchy. Highlighted cells indicate the best Euclidean embeddings as well as the Poincaré embeddings which achieve equal or better results. Bold numbers indicate absolute best results.

		Dimensionality					
		5	10	20	50	100	200
WORDNET Reconstruction	Euclidean	Rank MAP	3542.3 0.024	2286.9 0.059	1685.9 0.087	1281.7 0.140	1187.3 0.162
	Translational	Rank MAP	205.9 0.517	179.4 0.503	95.3 0.563	92.8 0.566	92.7 0.562
	Poincaré	Rank MAP	4.9 0.823	4.02 0.851	3.84 0.855	3.98 0.86	3.9 0.857
							3.83 0.87
WORDNET Link Pred.	Euclidean	Rank MAP	3311.1 0.024	2199.5 0.059	952.3 0.176	351.4 0.286	190.7 0.428
	Translational	Rank MAP	65.7 0.545	56.6 0.554	52.1 0.554	47.2 0.56	43.2 0.562
	Poincaré	Rank MAP	5.7 0.825	4.3 0.852	4.9 0.861	4.6 0.863	4.6 0.856
							4.6 0.855

Link Prediction To test generalization performance, we split the data into a train, validation and test set by randomly holding out observed links. Links in the validation and test set do not include the root or leaf nodes as these links would either be trivial to predict or impossible to predict reliably.

Furthermore, since we are interested in determining whether Poincaré embeddings are able to infer latent hierarchies, we do not embed these taxonomies in their clean form of a minimal tree. Instead, we embed their *transitive closure* such that the hierarchical structure is not directly visible from the raw data. The transitive closure of the WORDNET noun hierarchy consists of 82,115 nouns and 743,241 hypernymy relations. On this data, we then learn embeddings in both settings as follows: Let $\mathcal{D} = \{(u, v)\}$ be the set of observed hypernymy relations between noun pairs. We then learn embeddings of all symbols in \mathcal{D} such that related objects are close in the embedding space. In particular, we minimize the loss function

$$\mathcal{L}(\Theta) = \sum_{(u, v) \in \mathcal{D}} \log \frac{e^{-d(\mathbf{u}, \mathbf{v})}}{\sum_{v' \in \mathcal{N}(u)} e^{-d(\mathbf{u}, \mathbf{v}')}}, \quad (6)$$

where $\mathcal{N}(u) = \{v \mid (u, v) \notin \mathcal{D}\} \cup \{u\}$ is the set of negative examples for u (including u). For training, we randomly sample 10 negative examples per positive example. Equation (6) can be interpreted as a soft ranking loss where related objects should be closer than objects for which we didn't observe a relationship. This choice of loss function is motivated by the fact that we don't want to push symbols belonging to distinct subtrees arbitrarily far apart as their subtrees might still be close. Instead we simply want them to be farther apart than symbols with an observed relation.

We then evaluate the quality of the embeddings as it is commonly done for graph embeddings [6, 21]: For each observed relationship (u, v) , we rank its distance $d(\mathbf{u}, \mathbf{v})$ among the ground-truth negative examples for u , i.e., among the set $\{d(\mathbf{u}, \mathbf{v}') \mid (u, v') \notin \mathcal{D}\}$. In the Reconstruction setting, we evaluate the ranking on all nouns in the dataset. We then record the mean rank of v as well as the mean average precision (MAP) of the ranking. The results of these experiments are shown in Table 1. It can be seen that Poincaré embeddings are very successful in the embedding of large taxonomies – both with regard to their representation capacity and their generalization performance. In both settings, Poincaré embeddings achieve by far the best results and more so with exceptionally low-dimensional representations. Even compared to Translational embeddings, which have more information about the structure of the task, Poincaré embeddings show a greatly improved performance while using an embedding that is smaller by an order of magnitude. Furthermore, the results of Poincaré embeddings in the link prediction task are very robust with regard to an increased embedding dimension. We attribute this result to the structural bias of Poincaré embeddings, what could lead to reduced overfitting on this kind of data with a clear latent hierarchy. In Figure 2 we

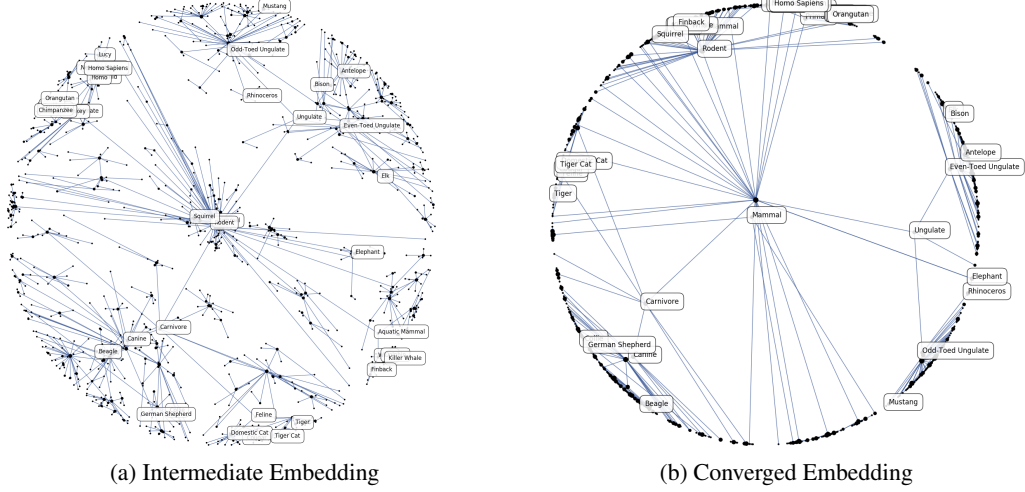


Figure 2: Two-dimensional Poincaré embeddings of transitive closure of the WORDNET mammals subtree. Ground-truth *is-a* relations of the original WORDNET tree are indicated via blue edges. A Poincaré embedding with $d = 5$ achieves mean rank 1.26 and MAP 0.927 on this subtree. (a) Intermediate embedding after 20 epochs. (b) Embeddings after convergence.

show additionally a visualization of a two-dimensional Poincaré embedding. For purpose of clarity, this embedding has been trained only on the mammals subtree of WORDNET.

4.2 Network Embeddings

Next, we evaluated the performance of Poincaré embeddings for link prediction in networks. Since edges in complex networks can often be explained via latent hierarchies over their nodes [8], we expect benefits of Poincaré embeddings both in terms representation size and generalization performance. We performed our experiments on four commonly used social networks, i.e, ASTROPH, CONDMAT, GRQC, and HEPH. These networks represent scientific collaborations such that there exists an undirected edge between two persons if they co-authored a paper. For these networks, we model the probability of an edge as proposed by Krioukov et al. [16] via the Fermi-Dirac distribution

$$P((u, v) = 1 \mid \Theta) = \frac{1}{e^{(d(u, v) - r)/t} + 1} \quad (7)$$

where $r > 0$ and $0 < t < 1$ are hyperparameters. Here, r corresponds to the radius around each point u such that points that are closer than r are likely to have an edge with u . The parameter t specifies the steepness of the logistic function. We then use the cross-entropy loss to learn the embeddings and sample negatives as described in Section 4.1.

For evaluation, we split each dataset randomly into train, validation, and test set. The hyperparameters r and t were tuned for each method on the validation set. Table 2 lists the MAP score of Poincaré and Euclidean embeddings on the test set for the hyperparameters with the best validation score. Additionally, we again list the reconstruction performance without missing data. Translational embeddings are not applicable to these datasets as they consist of undirected edges. It can be seen that Poincaré embeddings perform again very well on these datasets and – especially in the low-dimensional regime – outperform Euclidean embeddings.

4.3 Lexical Entailment

An interesting aspect of Poincaré embeddings is that they allow us to make graded assertions about hierarchical relationships as hierarchies are represented in a continuous space. We test this property on HYPERLEX [26], which is a gold standard resource for evaluating how well semantic models capture graded lexical entailment by quantifying to what *degree* X is a type of Y via ratings on a scale of $[0, 10]$. Using the noun part of HYPERLEX, which consists of 2163 rated noun pairs, we then evaluated how well Poincaré embeddings reflect these graded assertions. For this purpose, we

Table 2: Mean average precision for Reconstruction and Link Prediction on network data.

		Dimensionality							
		Reconstruction				Link Prediction			
		10	20	50	100	10	20	50	100
ASTROPH N=18,772; E=198,110	Euclidean	0.376	0.788	0.969	0.989	0.508	0.815	0.946	0.960
	Poincaré	0.703	0.897	0.982	0.990	0.671	0.860	0.977	0.988
CONDMAT N=23,133; E=93,497	Euclidean	0.356	0.860	0.991	0.998	0.308	0.617	0.725	0.736
	Poincaré	0.799	0.963	0.996	0.998	0.539	0.718	0.756	0.758
GRQC N=5,242; E=14,496	Euclidean	0.522	0.931	0.994	0.998	0.438	0.584	0.673	0.683
	Poincaré	0.990	0.999	0.999	0.999	0.660	0.691	0.695	0.697
HEPPH N=12,008; E=118,521	Euclidean	0.434	0.742	0.937	0.966	0.642	0.749	0.779	0.783
	Poincaré	0.811	0.960	0.994	0.997	0.683	0.743	0.770	0.774

Table 3: Spearman’s ρ for Lexical Entailment on HYPERLEX.

FR	SLQS-Sim	WN-Basic	WN-WuP	WN-LCh	Vis-ID	Euclidean	Poincaré	
ρ	0.283	0.229	0.240	0.214	0.214	0.253	0.389	0.512

used the Poincaré embeddings that were obtained in Section 4.1 by embedding WORDNET with a dimensionality $d = 5$. Note that these embeddings were not specifically trained on HYPERLEX. As a score function to determine to what extent $\text{is-a}(u, v)$ is true, we used:

$$\text{score}(\text{is-a}(u, v)) = -(1 + \alpha(\|v\| - \|u\|))d(u, v). \quad (8)$$

Here, the term $\alpha(\|v\| - \|u\|)$ acts as a penalty when v is lower in the embedding hierarchy, i.e., when v has a higher norm than u . The hyperparameter α determines the severity of the penalty. In our experiments we set $\alpha = 10^3$.

Using Equation (8), we scored all noun pairs in HYPERLEX and recorded Spearman’s rank correlation with the ground-truth ranking. The results of this experiment are shown in Table 3. It can be seen that the ranking based on Poincaré embeddings clearly outperforms all state-of-the-art methods evaluated in [26]. Methods in Table 3 that are prefixed with WN also use WORDNET as a basis and therefore are most comparable. The same embeddings also achieved a state-of-the-art accuracy of 0.86 on WBLESS [27, 14], which evaluates non-graded lexical entailment.

5 Discussion and Future Work

In this paper, we introduced Poincaré embeddings for learning representations of symbolic data and showed how they can simultaneously learn the similarity and the hierarchy of objects. Furthermore, we proposed an efficient algorithm to compute the embeddings and showed experimentally that Poincaré embeddings provide important advantages over Euclidean embeddings on hierarchical data: First, Poincaré embeddings enable parsimonious representations what allows us to learn high-quality embeddings of large-scale taxonomies. Second, excellent link prediction results indicate that hyperbolic geometry can introduce an important structural bias for the embedding of complex symbolic data. Third, state-of-the-art results for predicting lexical entailment suggest that the hierarchy in the embedding space corresponds well to the underlying semantics of the data.

The main focus of this work was to evaluate the general properties of hyperbolic geometry for the embedding of symbolic data. In future work, we intend to, both, expand the applications of Poincaré embeddings – for instance to multi-relational data – and also to derive models that are more strongly tailored to specific applications such as word embeddings. Furthermore, we have shown that natural gradient based optimization already produces very good embeddings and scales to large datasets. We expect that a full Riemannian optimization approach can further increase the quality of the embeddings and lead to faster convergence.

References

- [1] Aaron B Adcock, Blair D Sullivan, and Michael W Mahoney. Tree-like structure in large social and information networks. In *Data Mining (ICDM), 2013 IEEE 13th International Conference on*, pages 1–10. IEEE, 2013.
- [2] Shun-ichi Amari. Natural gradient works efficiently in learning. 10(2):251–276, 1998.
- [3] M Boguñá, F Papadopoulos, and D Krioukov. Sustaining the internet with hyperbolic mapping. 1:62, 2010.
- [4] Piotr Bojanowski, Edouard Grave, Armand Joulin, and Tomas Mikolov. Enriching word vectors with subword information. 2016.
- [5] Silvere Bonnabel. Stochastic gradient descent on riemannian manifolds. 58(9):2217–2229, 2013.
- [6] Antoine Bordes, Nicolas Usunier, Alberto García-Durán, Jason Weston, and Oksana Yakhnenko. Translating embeddings for modeling multi-relational data. In *Advances in Neural Information Processing Systems 26*, pages 2787–2795, 2013.
- [7] Guillaume Bouchard, Sameer Singh, and Theo Trouillon. On approximate reasoning capabilities of low-rank vector spaces. 2015.
- [8] Aaron Clauset, Cristopher Moore, and Mark EJ Newman. Hierarchical structure and the prediction of missing links in networks. 453(7191):98–101, 2008.
- [9] John Rupert Firth. A synopsis of linguistic theory, 1930-1955. 1957.
- [10] Mikhael Gromov. Hyperbolic groups. In *Essays in group theory*, pages 75–263. Springer, 1987.
- [11] Aditya Grover and Jure Leskovec. node2vec: Scalable feature learning for networks. In *Proceedings of the 22nd ACM SIGKDD International Conference on Knowledge Discovery and Data Mining*, pages 855–864. ACM, 2016.
- [12] Zellig S Harris. Distributional structure. 10(2-3):146–162, 1954.
- [13] Peter D Hoff, Adrian E Raftery, and Mark S Handcock. Latent space approaches to social network analysis. 97(460):1090–1098, 2002.
- [14] Douwe Kiela, Laura Rimell, Ivan Vulic, and Stephen Clark. Exploiting image generality for lexical entailment detection. In *Proceedings of the 53rd Annual Meeting of the Association for Computational Linguistics (ACL 2015)*, pages 119–124. ACL, 2015.
- [15] Robert Kleinberg. Geographic routing using hyperbolic space. In *INFOCOM 2007. 26th IEEE International Conference on Computer Communications*. IEEE, pages 1902–1909. IEEE, 2007.
- [16] Dmitri Krioukov, Fragkiskos Papadopoulos, Maksim Kitsak, Amin Vahdat, and Marián Boguná. Hyperbolic geometry of complex networks. 82(3):036106, 2010.
- [17] Tomas Mikolov, Ilya Sutskever, Kai Chen, Greg Corrado, and Jeffrey Dean. Distributed representations of words and phrases and their compositionality. abs/1310.4546, 2013.
- [18] George Miller and Christiane Fellbaum. Wordnet: An electronic lexical database, 1998.
- [19] Maximilian Nickel, Volker Tresp, and Hans-Peter Kriegel. A three-way model for collective learning on multi-relational data. In *Proceedings of the 28th International Conference on Machine Learning, ICML 2011, Bellevue, Washington, USA, June 28 - July 2, 2011*, pages 809–816, 2011.
- [20] Maximilian Nickel, Xueyan Jiang, and Volker Tresp. Reducing the rank in relational factorization models by including observable patterns. In *Advances in Neural Information Processing Systems 27*, pages 1179–1187, 2014.
- [21] Maximilian Nickel, Lorenzo Rosasco, and Tomaso A. Poggio. Holographic embeddings of knowledge graphs. In *Proceedings of the Thirtieth AAAI Conference on Artificial Intelligence, February 12-17, 2016, Phoenix, Arizona, USA.*, pages 1955–1961, 2016.
- [22] Jeffrey Pennington, Richard Socher, and Christopher D Manning. Glove: Global vectors for word representation. In *EMNLP*, volume 14, pages 1532–1543, 2014.
- [23] Erzsébet Ravasz and Albert-László Barabási. Hierarchical organization in complex networks. 67(2):026112, 2003.

- [24] Benjamin Recht, Christopher Ré, Stephen J. Wright, and Feng Niu. Hogwild: A lock-free approach to parallelizing stochastic gradient descent. In *Advances in Neural Information Processing Systems 24*, pages 693–701, 2011.
- [25] Mark Steyvers and Joshua B Tenenbaum. The large-scale structure of semantic networks: Statistical analyses and a model of semantic growth. 29(1):41–78, 2005.
- [26] Ivan Vulić, Daniela Gerz, Douwe Kiela, Felix Hill, and Anna Korhonen. Hyperlex: A large-scale evaluation of graded lexical entailment. 2016.
- [27] Julie Weeds, Daoud Clarke, Jeremy Reffin, David Weir, and Bill Keller. Learning to distinguish hypernyms and co-hyponyms. In *Proceedings of COLING 2014, the 25th International Conference on Computational Linguistics: Technical Papers*, pages 2249–2259. Dublin City University and Association for Computational Linguistics, 2014.
- [28] Hongyi Zhang, Sashank J. Reddi, and Suvrit Sra. Riemannian SVRG: fast stochastic optimization on riemannian manifolds. In *Advances in Neural Information Processing Systems 29*, pages 4592–4600, 2016.
- [29] George Kingsley Zipf. *Human Behaviour and the Principle of Least Effort: an Introduction to Human Ecology*. Addison-Wesley, 1949.